Erbium Spectroscopy and 1.5-μm Emission in $KGd(WO_4)_2$: Er,Yb Single Crystals

Xavier Mateos, Maria Cinta Pujol, Frank Güell, Miguel Galán, Rosa Maria Solé, Josefina Gavaldà, Magdalena Aguiló, Jaume Massons, and Francesc Díaz

***Abstract*—We grew good-optical-quality $KGd(WO_4)_2$ single crystals doped with erbium and ytterbium ions at several concentrations of dopants using the top-seeded-solution growth slow-cooling method (TSSG). We performed the spectroscopic characterization of this material related to the 1.5-μm infrared emission of erbium which is interesting for laser applications. To do this, we carried out polarized optical absorption at room temperature (RT) and at low temperature (6 K) and performed luminescence studies of the emission and lifetime. We obtained the 1.5-μm emission of erbium after selective laser pump excitation of the ytterbium ion and energy transfer between the two ions. The maximum emission cross section for 1.5 μm was about 2.56×10^{-20} cm^2 for the polarization of light with the electric field parallel to the N_m principal optical direction. This value was higher than for other erbium-doped materials with application in solid-state lasers such as $LiYF_4$: Er(YLF : Er), $Y_3Al_5O_{12}$: Er(YAG : Er), $YAlO_3$: Er, and Al_2O_3 : Er.**

***Index Terms*—Erbium, $KGd(WO_4)_2$, solid-state laser, spectroscopy, ytterbium.**

I. Introduction

MANY researchers into laser systems focus on lasers operating in the infrared spectral range, especially around 1.5 and 3 μm (6667 and 3333 cm^{-1}) for use in, for example, optical communications, medicine, and light detection and ranging (LIDAR) [1], [2]. Of these, solid-state lasers are preferred for most applications because they are robust, relatively simple to fabricate, and easy to use [3], [4]. The availability of laser diodes emitting in the 0.55–1.9 μm (18182-5263 cm^{-1}) spectral range makes diode-pumped solid-state-lasers clearly interesting.

Some excited energy levels of erbium for the $4f$ shell can be used to achieve luminescence from which stimulated emission of radiation is generated. The erbium ion is suitable for obtaining laser radiation in the near-infrared region after diode pumping because of its $^4I_{11/2}$ energy level to absorb the pump radiation and its $^4I_{13/2}$ energy level to emit to the ground state (1.5-μm emission). Its absorption band between 0.9 and 1.1 μm (11111-9091 cm^{-1}), corresponding to the $^4I_{11/2}$ energy level, is in the easily available diode-laser emission range, but its low absorption cross section in the above-mentioned spectral range limits pump efficiency. Ytterbium ions are widely used as sensitizer ions for increasing the absorption of light. Ytterbium ions posses a high absorption cross section in the above-mentioned spectral range and its $^2F_{5/2}$ energy level overlaps in energy with the $^4I_{11/2}$ energy level of erbium. This energy overlap derives to a very good resonant energy transfer between these two ions and the consequently greater efficiency of erbium luminescence generation. All of these advantages make ytterbium an ideal sensitizer ion of erbium [5]. The 1.5-μm (6667 cm^{-1}) erbium emission comprises a very efficient three-level laser system.

The low-temperature monoclinic phase of potassium rare-earth tungstates, $KRE(WO_4)_2$ (RE=rare earth), which is widely known as host for active ions to constitute a solid-state laser material, can be doped with optical active lanthanide ions even at high concentrations [6]. Tungstates are the most efficient of all known inorganic laser materials for stimulating emission at small pumping energies [7]. $KRE(WO_4)_2$ hosts have a high nonlinear susceptibility of the third order, so they are promising Raman-active media [8].

Potassium gadolinium tungstate doped with erbium and ytterbium ions $KGd(WO_4)_2$: Er-Yb (hereafter KGW:Er-Yb) has spectroscopic properties that can be interesting to achieve 1.5-μm (6667-cm^{-1}) infrared laser emission via energy transfer from ytterbium to erbium.

KGW has a monoclinic crystallographic structure with space group C2/c and lattice parameters $a = 10.652(4)$ Å, $b = 10.374(6)$ Å, $c = 7.582(2)$ Å, and $\beta = 130.80(2)^\circ$ [9] with $Z = 4$. The three principal optical directions of monoclinic KGW are located along the crystal as follows. The principal optical axis N_g with maximum refractive index is at 21.5° in clockwise rotation with respect to the $\boldsymbol{c}$ crystallographic axis and the $\boldsymbol{b}$ positive axis pointing toward the observer. The principal optical axis with intermediate refractive index N_m is at 62.3° with respect to the $\boldsymbol{a}$ crystallographic axis and N_g and N_m in the a–c plane. Finally, the N_p principal axis is parallel to the $\boldsymbol{b}$ crystallographic axis [10]. The optical-quality polished samples we used in our study were prisms cut with their faces perpendicular to the three principal optical axes.

In this study, we describe the growth of KGW single crystals doped with erbium and ytterbium ions (KGW:Er-Yb) and study the spectroscopic properties of erbium ions sensitized by ytterbium. We study the polarized optical absorption at room-temperature (RT) and 6 K, the near-infrared photoluminescence around 1.5 μm (6667 cm^{-1}), also at RT and 6 K, and, finally, the decay curves at several concentration of erbium and ytterbium. We used the Reciprocity method to calculate the $^4I_{13/2} \rightarrow {}^4I_{15/2}$ emission cross section from the absorption cross-section line shape.

Manuscript received September 10, 2003; revised February 3, 2004. This work was supported by CICyT under Project MAT2002-04603-C05-03 and Project FiT-07000-2002-461 and CIRIT under Project 2001SGR00317.

X. Mateos, M. C. Pujol, F. Güell, R. M. Solé, J. Gavaldà, M. Aguiló, J. Massons, and F. Díaz are with Física i Cristal lografia de Materials (FiCMA), Universitat Rovira i Virgili, 43005 Tarragona, Spain.

M. Galán is with MONOCROM S.L., Polígon Roquetes II, Vilanova i la Geltrú, Barcelona, Spain.

Digital Object Identifier 10.1109/JQE.2004.828238

TABLE I
CRYSTAL GROWTH DATA OF THE KGW:Er, Yb SINGLE CRYSTALS AT SEVERAL ERBIUM AND YTTERBIUM CONCENTRATIONS

A	B	C	D	E	F	G	H	I	J	K
0.5%Er , 0.5%Yb	0.1 0.05	2 10	1.01	50	few	8.0	8.5	4.0	0.004	0.004
1.5%Er , 1.5%Yb	0.1 0.05	2 10	1.04	47	few	7.0	8.0	4.0	0.012	0.016
2.5%Er , 2.5%Yb	0.1 0.05	1 10	1.20	52	few	8.5	10.5	3.0	0.020	0.022
5%Er , 5%Yb	0.1 0.05	2 10	1.25	51	few	9.0	8.5	3.0	0.043	0.038
0.5%Er , 1.5%Yb	0.1 0.05	2 10	3.98	181	-	15.0	9.0	6.5	0.003	0.020
0.5%Er , 2.5%Yb	0.1 0.05	2 10	4.25	193	-	13.0	10.0	7.0	0.006	0.028
0.5%Er , 5.0%Yb	0.1 0.05	2 10	4.50	201	-	12.0	12.0	7.0	0.003	0.035
0.5%Er , 7.5%Yb	0.1 0.05	2 9	4.83	242	-	12.5	11.0	7.5	0.002	0.059
0.5%Er , 10%Yb	0.1 0.05	2 11	4.75	198	-	14.0	12.0	6.0	0.004	0.060
0.5%Er , 15%Yb	0.1 0.05	2 9	3.77	189	crack	15.0	10.0	5.0	0.004	0.105
1.44%Er , 2.51%Yb	0.1 0.05	2 10	3.99	182	-	13.0	11.0	7.0	0.014	0.031
1.8%Er , 5.0%Yb	0.1 0.05	2 6	3.29	183	-	12.0	11.0	8.0	0.010	0.034
1.47%Er , 7.5%Yb	0.1 0.05	2 10	5.09	182	few	-	-	-	0.009	0.047
1.5%Er , 10%Yb	0.1 0.05	2 10	4.24	189	-	14.0	9.5	6.0	0.010	0.064
2.5%Er , 5.0%Yb	0.1 0.05	2 12	5.08	195	-	16.0	9.5	6.5	0.022	0.055
2.5%Er , 7.5%Yb	0.1 0.05	2 9	3.89	195	-	14.0	10.0	5.0	0.019	0.066
2.5%Er , 10%Yb	0.1 0.05	2 10.5	4.21	183	-	14.0	8.5	8.0	0.019	0.087

A: Dopant atomic percentage of substitution in solution with respect to the gadolinium. B: Cooling rate, K/h. C: Cooling interval, K. D: Crystal weight, g. E: Growth rate ($\times 10^{-4}$), g/h. F: Inclusions/defects. G: Crystal dimensions along the c direction, mm. H: Crystal dimensions along the a^* direction, mm. I: Crystal dimensions along the b direction, mm. J[a]: x in the crystal $[KGd_{1-x-y}Er_xYb_y(WO_4)_2]$. K[a]: y in the crystal $[KGd_{1-x-y}Er_xYb_y(WO_4)_2]$.

[a] The substitution level of Gd^{3+} by Er^{3+} and Yb^{3+} was determined by EPMA.

II. EXPERIMENTAL TECHNIQUES

Powdered precursors of KGW:Er-Yb single crystals were K_2CO_3, Gd_2O_3, Er_2O_3, Yb_2O_3, and WO_3 (Fluka, 99.9% pure). These were used to synthesize these types of single crystals at several erbium and ytterbium concentrations, $KGd_{1-x-y}Er_xYb_y(WO_4)_2$, with a binary solution composition of 11.5 mol.%solute/88.5 mol.%solvent. We used the top-seeded-solution growth slow-cooling method (TSSG) with $K_2W_2O_7$ as a solvent because this does not introduce foreign ions and because its melting point is low. Previous studies [11] of single-doped KGW: Ln^{3+} crystal growth have shown that parallelepipedic b-oriented seeds improve the rate of crystal growth and produce inclusion-free crystals than other crystallographic orientations. We therefore used our previously described method to grow the crystals [12].

We determined the concentration of erbium and ytterbium ions in the crystals by electron-probe microanalysis (EPMA) with Cameca SX 50 equipment.

We performed the polarized optical absorption experiments on a sample of 1KGW:Er-Yb (0.5%-0.5%) with a concentration of 1.44×10^{19} and 1.73×10^{19} at/cm^3 for erbium and ytterbium ions, respectively, because with these concentrations we achieved good resolution without saturating the detector.

These spectra were carried out at RT and 6 K with polarized light parallel to the N_g, N_m, and N_p principal optical directions. The measurements were taken with a VARIAN CARY-5E-UV-VIS-NIR 500Scan Spectrophotometer and a Glan-Taylor polarizer. Cryogenic temperatures were obtained with a Leybold RDK 6-320 cycle helium cryostat.

We did the photoluminescence experiments with a BMI OPO pumped by the third harmonic of a seeded BMI SAGA YAG:Nd laser. Pulses of 15 mJ (duration: 7 ns; repetition rate: 10 Hz) were achieved with a Gaussian beam profile. Fluorescence was dispersed through a HR460 Jobin Yvon-Spex monochromator (focal length 460 mm, f/5.3, spectral resolution 0.05 nm/mm) and detected by a cooled Hamamatsu R5509-72 NIR photomultiplier. We analyzed the luminescence signal using a EG&G 7265DSP lock-in amplifier. Low-temperature luminescence experiments were done by means of Oxford CCC1104 closed cycle helium cryostat.

The sample was KGW:Er-Yb (2.5%–7.5%) with a concentration of 1.20×10^{20} and 4.16×10^{20} at/cm^3 for erbium and ytterbium, respectively. We used a different concentration of dopant from the one for the absorption experiments because, at this concentration, infrared emission intensity was higher.

To analyze the behavior of the lifetime of the $^4I_{13/2}$ energy level of erbium, we took lifetime measurements of this energy level at several erbium and ytterbium concentrations using the averaging facilities of a computer-controlled Tektronix TDS-714 digital oscilloscope.

The Reciprocity method [13] is normally used to calculate the emission cross section of an optical transition from the optical absorption cross-section line shape at RT of a particular energy level. Absorption and emission processes are characterized by their absorption and emission cross sections (σ_{abs}, σ_e), respectively. From the energies and degeneracies of the upper and lower energy levels, we can find a mathematical expression that contains a direct relationship between these two cross sections to calculate the emission cross section. The Reciprocity calculation is based on

$$\sigma_e(\upsilon)=\sigma_{abs}(\upsilon)\frac{Z_l}{Z_u}\exp\left[\frac{(E_{zl}-h\upsilon)}{kT}\right] \tag{1}$$

where σ_e is the emission cross section to be calculated as a function of the frequency (or wavelength) and σ_{abs} is the absorption cross section obtained from the RT optical absorption, which in our case is the optical absorption of the $^4I_{15/2}\rightarrow{}^4I_{13/2}$ transition. The E_{zl} is the 'zero-line,' or the energy separation, derived from the crystal field component. This is between the lowest energy sublevel of the excited energy level (upper) and the lowest energy sublevel of the ground level (lower). k is Boltzman's constant and h is Planck's constant. Finally, Z_u and Z_l are the partition functions of the upper and lower energy levels, respectively, calculated from

$$Z_{u,l}=\sum_k d_k\exp\left(-\frac{E_k}{(kT)}\right) \tag{2}$$

where d_k and E_k are the degeneracies and the energies of each sublevel of the upper and lower energy levels involved in the system, obtained from the 6 K optical absorption.

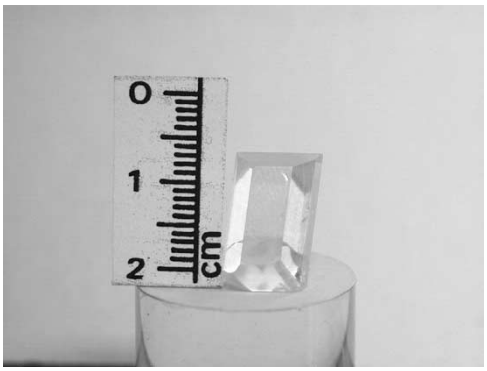

Fig. 1. Photograph of a KGW:Er-Yb single crystal.

Light amplification [14] is expected when the emitted light is higher than the absorption at the same wavelength. This condition can be described by

$$\sigma_{gain}=P\sigma_e-(1-P)\sigma_{abs} \tag{3}$$

where σ_{gain} is the gain (effective) emission cross section, σ_e is the calculated emission cross section, σ_{abs} is the absorption cross section, and P is the population inversion rate.

III. Results and Discussion

A. Crystal Growth

We grew good-optical-quality KGW:Er-Yb single crystals at several erbium and ytterbium concentrations by the TSSG method. Table I gives information about crystal growth, e.g., dopant solution composition, cooling rate, cooling interval, crystal dimensions, and crystal composition. The saturation temperature was between 1178 K and 1189 K. The seed orientation was along the $\boldsymbol{b}$ crystallographic direction in all cases. We grew some crystals under different conditions, 50 g of solution for the first four crystals in Table I and 200 g for the rest of them. For this, some parameters changed. The cooling rate was typically 0.1 K/h for the first two degrees of the cooling interval and 0.05 K/h for the second ten degrees of the cooling interval. In some experiences, the second cooling interval was slightly changed, as Table I shows. The rotation of the seed during the crystal growth was 40 rpm in all cases. We noted that, when the ytterbium concentration increased, the saturation temperature slightly decreased. The distribution coefficient of the dopant ions, measured by EPMA, was around unity, which means that the stoichiometry of the solute in the crystal was conserved.

Fig. 1 shows a photograph of a KGW:Er-Yb single crystal that is large enough for us to perform our spectroscopic studies.

B. Optical Absorption

We performed the polarized optical absorption of erbium and ytterbium ions in a KGW host at RT and 6 K. We used a KGW:Er-Yb single crystal for the optical absorption experiments with a concentration of ions of 1.44×10^{19} at./cm^3 for erbium and 1.73×10^{19} at./cm^3 for ytterbium. The optical orientation of the sample was determined using a Fedorov table. A sample 2.21 mm thick was used to analyze the anisotropic

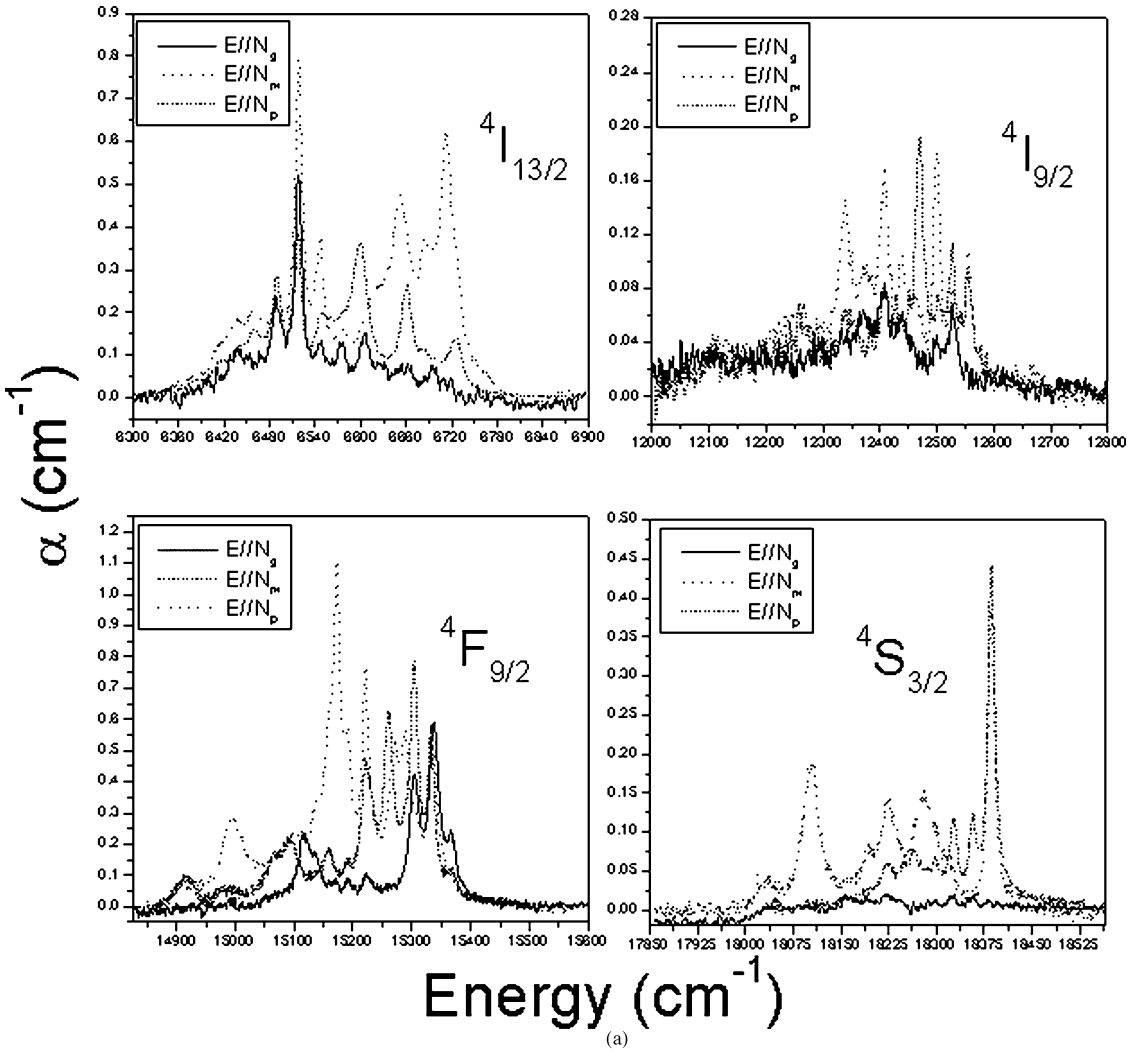

Fig. 2. (a) Polarized optical absorption coefficient of the excited energy levels of erbium in KGW:Er-Yb at RT in the 1587-540-nm (6300–18 500 cm^{-1}) spectral range.

behavior with the electric field of the incident radiation parallel to the N_g and N_m principal optical directions. The sample used to analyze the $E//N_g$ and $E//N_p$ directions was 2.71 mm thick. Fig. 2(a) and (b) show the RT polarized optical absorption of erbium in this host, except for the $^4I_{11/2}$ excited energy level of erbium, which overlapped with the $^2F_{5/2}$ excited energy level of ytterbium, which will be discussed later.

For studying the 1.5-μm infrared emission of erbium, the most interesting excited energy levels are $^4I_{13/2}$, because this is the starting energy level for this emission, and $^4I_{11/2}$ because this overlaps in energy with the $^2F_{5/2}$ excited energy level of ytterbium, where the energy transfer takes place.

Fig. 3 shows the polarized optical absorption of erbium in KGW:Er-Yb in the 1587-1449-nm (6300–6900 cm^{-1}) range, which is the spectral range of the $^4I_{13/2}$ energy level of erbium, and where the 1.5-μm emission takes place. Note the high anisotropy contribution of the host: the most intense absorption is obtained for the $E//N_m$ direction, whereas the least intense is $E//N_g$. Moreover, this energy level presents a high-absorption cross section. The value is maximum (2.49×10^{-20} cm^2) for the N_m principal optical direction at 1534 nm (6519 cm^{-1}), which is clearly higher than those for other erbium-doped laser materials such as YLF, YAG, $YAlO_3$, Al_2O_3 [15], and fluoride phosphate glass [16]. Fig. 3 also compares the absorption cross section for each principal optical direction of the crystal with the emission cross section. We calculated the emission cross section using the Reciprocity method from the absorption cross-section line shape. We can see that the calculated maximum emission cross section is 2.56×10^{-20} at 1534 nm (6519 cm^{-1}) for the N_m principal optical direction. This emission cross section is also higher than that of the above-mentioned erbium-doped laser materials.

We calculated the optical gain for several population inversion rates, i.e., 40%, 50%, and 60%, from the calculated emission cross-section spectrum for $E//N_m$, because it was the most intense. Fig. 4 shows that the gain is produced in the 1587-1527-nm region (6301–6549 cm^{-1}) for a population inversion level of 40%. The higher energy limit of this interval increased by increasing the population inversion level, reaching up to 1487 nm (6725 cm^{-1}) for a population inversion level of 60%. For this ,level the maximum gain cross section value was of 1.54×10^{-20} cm^2 at 1534 nm (6519 cm^{-1}). At this point, we expect to find the maximum light amplification in future laser experiments for this emission.

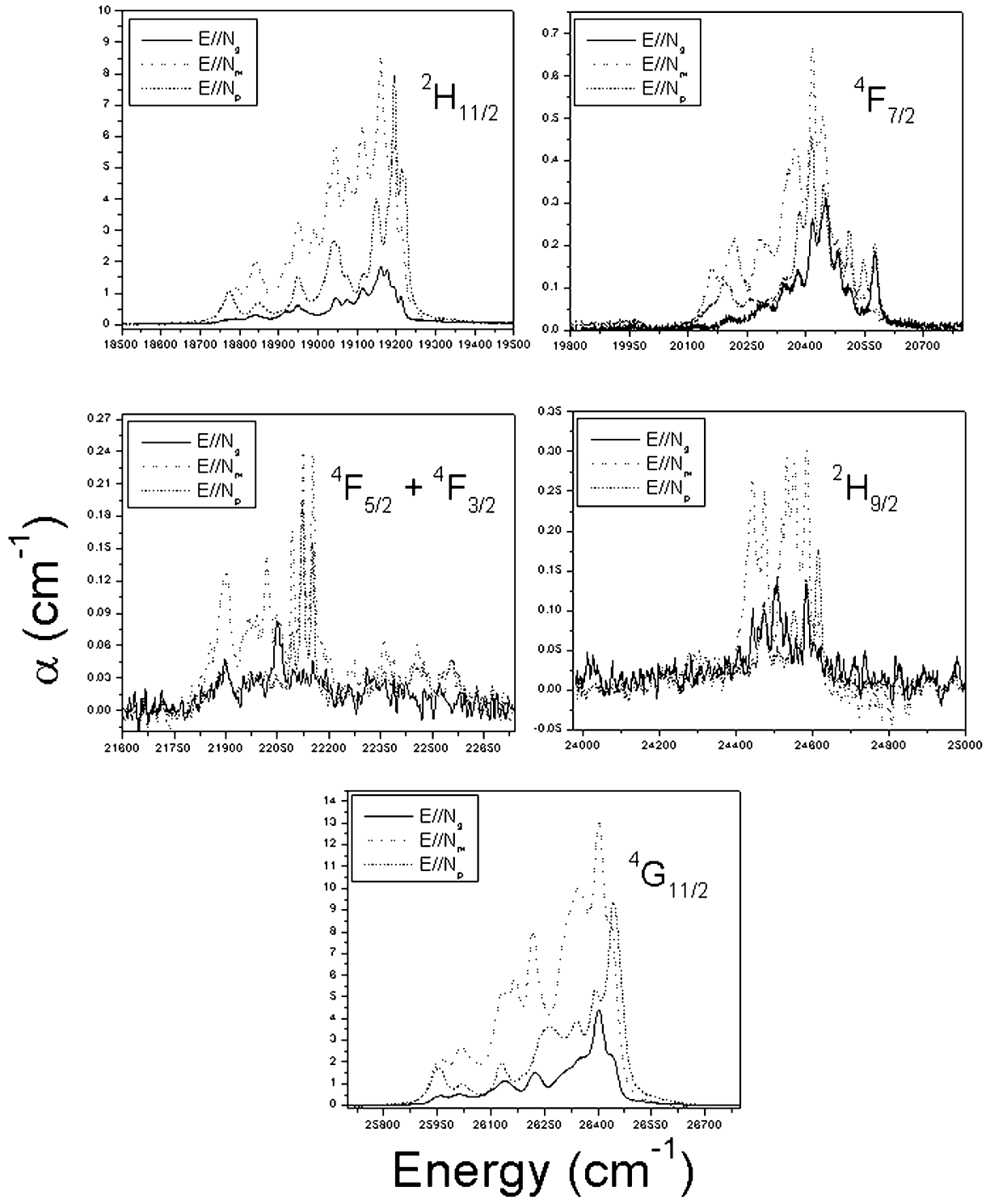

(b)

Fig. 2. *(Continued.)* (b) Polarized optical absorption coefficient of the excited energy levels of erbium in KGW:Er-Yb at RT in the 540-373-nm (18500–26 775 cm^{-1}) spectral range.

The other important excited energy level of erbium is $^4I_{11/2}$, which overlaps in energy with the $^2F_{5/2}$ energy level of ytterbium favoring the energy transfer between the two ions. Fig. 5 shows these overlapped energy levels at RT for the three principal optical directions. In this spectrum, the optical anisotropy induced by the host and the maximum absorption cross section of 11.6×10^{-20} cm^2 at 980.8 nm (10196 cm^{-1}) are more noticeable. This value agrees well with those we previously found in $KYb(WO_4)_2$ single crystal [17] and what Kuleshov *et al.* found in ytterbium-doped $KGd(WO_4)_2$ and $KY(WO_4)_2$ [18].

We made complementary studies of polarized optical absorption at 6 K on the erbium-ytterbium-doped KGW in the 1.7-0.3-μm (5880–33 300 cm^{-1}) range to determine the sublevels of the excited energy levels caused by the elimi-

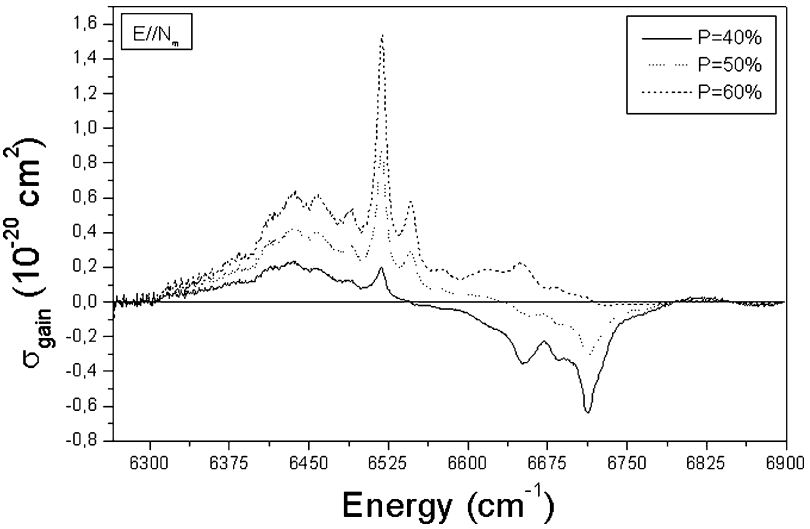

Fig. 4. Gain cross section of the 1.5-μm emission of erbium in KGW:Er-Yb at RT for the $E//N_m$ polarization at several inversion population rates.

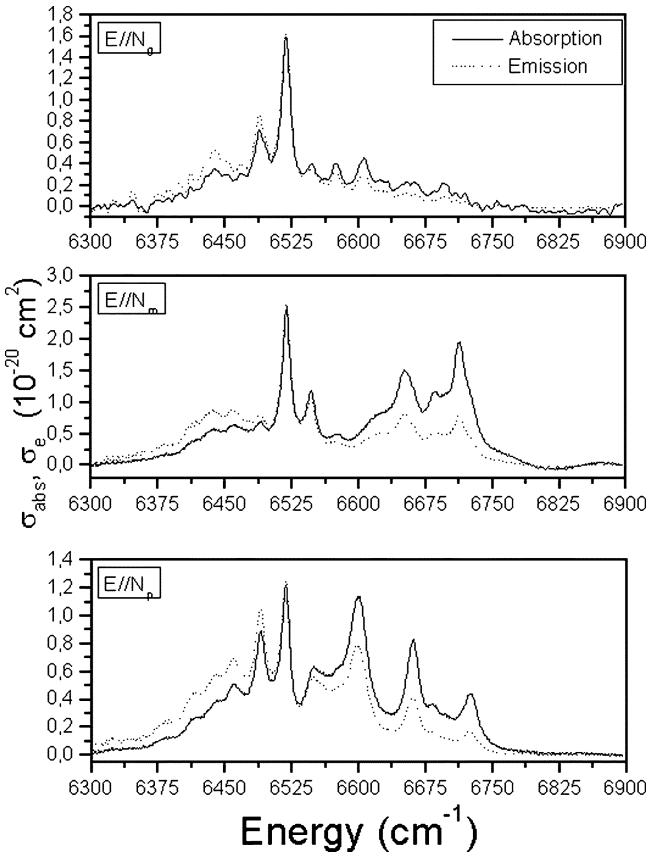

Fig. 3. Polarized absorption cross section and calculated emission cross section of the 1.5-μm emission of erbium in KGW:Er-Yb at RT in the 1587-1449-nm (6300–6900 cm^{-1}) spectral range.

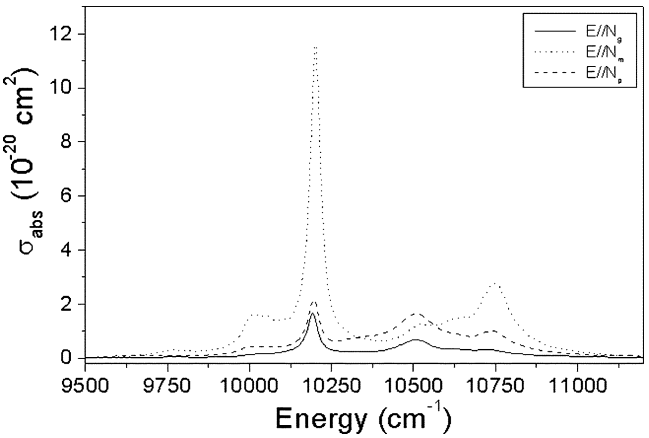

Fig. 5. Polarized optical absorption cross section of the overlapped energy levels of erbium and ytterbium performed at RT.

nation of the thermal population in the energy levels and the elimination of the thermal lattice vibrations. We assumed that, for erbium and ytterbium, at 6 K only the lowest sublevel of the ground state ($^4\mathrm{I}_{15/2}$ for erbium and $^2\mathrm{F}_{7/2}$ for ytterbium) were populated and that they were split by the local field of the ions surrounding the erbium and ytterbium dopants. The shape of the absorption lines should therefore reflect the transition probabilities from the lowest sublevel of the ground level to the sublevels of each excited energy levels of erbium. Fig. 6(a) and (b) shows the polarized optical absorption spectra at 6 K of all of the excited energy levels of erbium found in KGW crystal, except for $^4\mathrm{I}_{11/2}$, because this overlapped with the $^2\mathrm{F}_{5/2}$ level of ytterbium. The sample was the same as the one used at RT for the 1590-1450-μm (6300–6900 cm^{-1}) spectral range. The crystal field splits these manifolds into $(2J+1)/2$ sublevels, which is in agreement with the splitting expected by the crystalline field into the maximum number of Kramers levels (hereafter, sublevels) due to the odd number of electrons of erbium and the low symmetry where erbium is located (C_2, binary axes). Note from the spectra that the anisotropic contribution of the host was as at RT, the optical transitions ($^4\mathrm{I}_{15/2} \rightarrow {}^4\mathrm{G}_{11/2}$ and $^4\mathrm{I}_{15/2} \rightarrow {}^2\mathrm{H}_{11/2}$) were hypersensitive due to the large oscillator strength, and the signal at 6 K was much more intense than the signals at RT.

To describe accurately the energy overlap between Er and Yb, we measured the 6 K optical absorption of erbium and ytterbium in the region of interest in two different samples, KGW:Er (1%) and KGW:Yb (1%). Fig. 7 shows this overlap at 6 K for these two samples. Note that one peak is overlapped at 980.8 nm (10196 cm^{-1}) only at 6 K. The others are overlapped at RT (see Fig. 5).

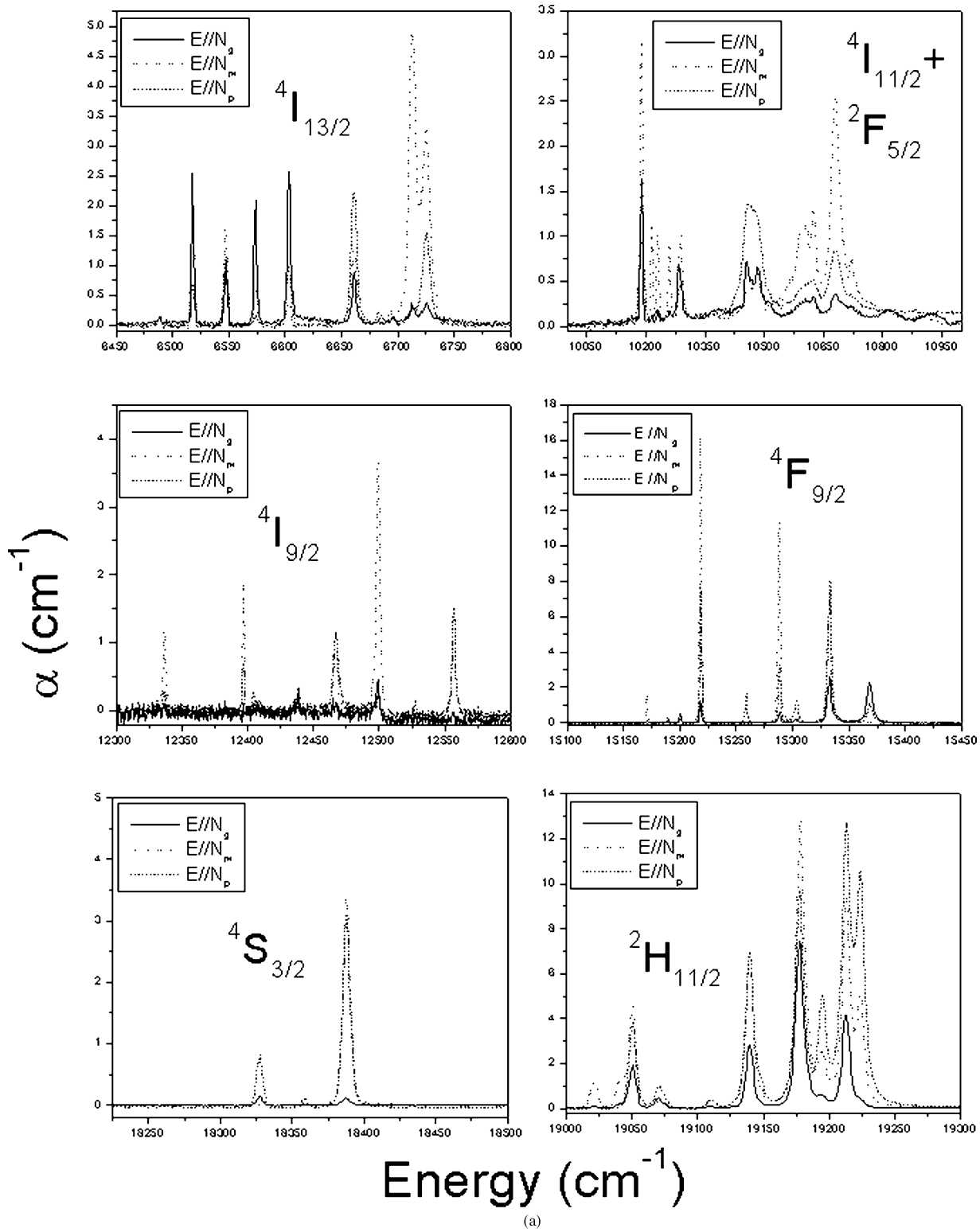

(a)

Fig. 6. (a) Polarized optical absorption coefficient of the excited energy levels of erbium in KGW:Er-Yb at 6 K in the 1550-518-nm (6450–19 300 cm^{-1}) spectral range.

Table II shows the splitting of the excited energy levels of erbium in KGW:Er-Yb single crystals. In all cases, the excited energy levels show the expected number of sublevels. For the $^4I_{15/2} \rightarrow {}^4I_{13/2}$ infrared transition, we expected the number of signals to be seven and the energy difference between the first and second energy sublevels was 30 cm^{-1}. We later used this energy difference to calculate the splitting of the ground energy level. These values are similar to those for erbium in similar materials, such as KYbW:Er [19], KGW:Er [10], and KYW:Er [20].

We compared the splitting of each energy level into its sublevels of erbium in KGW with the splitting found previously in KYbW:Er [19]. The splitting in KYbW crystals was slightly greater than in KGW crystals, showing that the crystal field

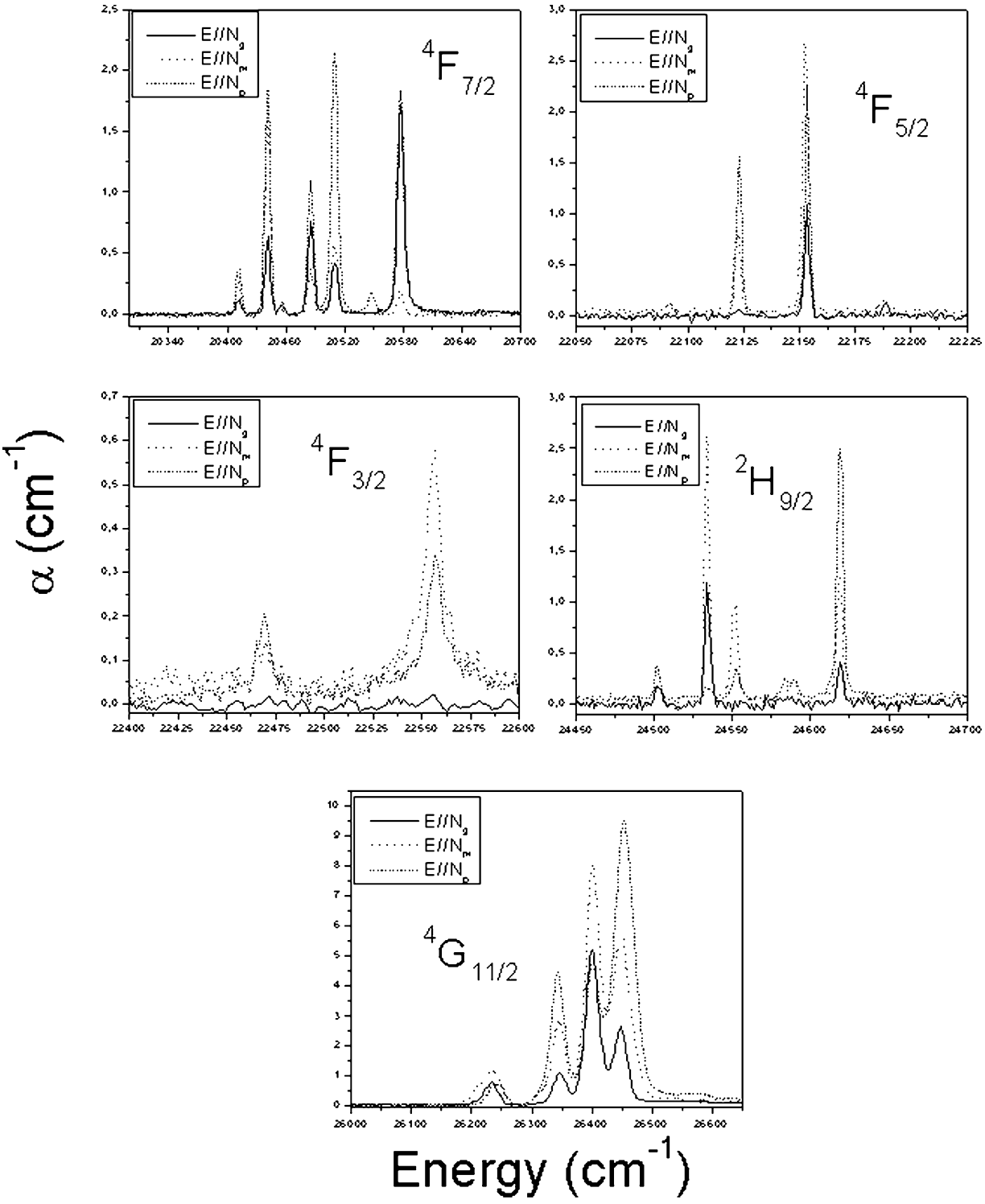

(b)

Fig. 6. *(Continued.)* (b) Polarized optical absorption coefficient of the excited energy levels of erbium in KGW:Er-Yb at 6 K in the 490-375-nm (20300–26 650 cm^{-1}) spectral range.

of KYbW was stronger than in KGW, which agrees well with the fact that the interatomic distances Yb-Yb in KYbW were smaller than the corresponding Gd-Gd distances in KGW [9], [21], [22]. Also, the previously calculated Judd–Ofelt parameters of erbium in KYbW [19] and in KGW [10], showed the influence of this crystal field, where the Judd–Ofelt parameters of KYbW were larger than those of KGW.

C. Luminescence

The aim of our luminescence studies was to determine the emission properties of erbium ion at RT around 1.5 μm sensitized by ytterbium, and the determination of the energy sublevels of the ground energy level of erbium in this host, by means of the 6 K emission experiments.

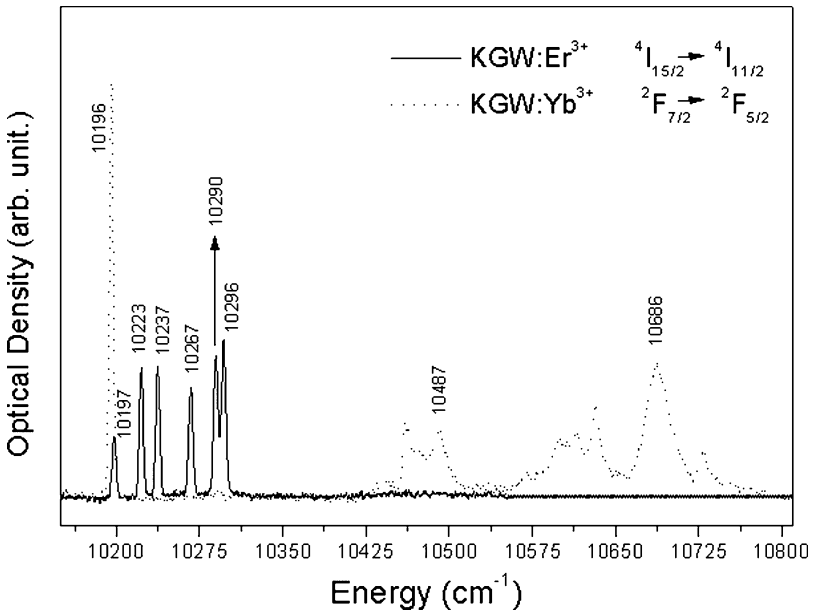

Fig. 7. Comparison of the optical absorption density of the overlapped energy levels of erbium and ytterbium in KGW:Er and KGW:Yb performed at 6 K.

TABLE II
SPLITTING OF THE EXCITED ENERGY LEVELS OF ERBIUM IN KGW:Er, Yb SINGLE CRYSTALS

$^{2S+1}L_J$	Sublevels energy position (cm^{-1})
$^4I_{13/2}$	6517, 6547, 6574, 6603, 6662, 6713, 6725.
$^4I_{9/2}$	12337, 12438, 12467, 12499, 12557.
$^4F_{9/2}$	15170 15200, 15218, 15288, 15333.
$^4S_{3/2}$	18327, 18388.
$^2H_{11/2}$	19050, 19072, 19139, 19178, 19213, 19224.
$^4F_{7/2}$	20441, 20485, 20510, 20577.
$^4F_{5/2}$	22122, 22153, 22189.
$^4F_{3/2}$	22469, 22556.
$^2H_{9/2}$	24501, 24533, 24551, 24582, 246199.
$^4G_{11/2}$	26231, 26344, 26401, 26438, 26449, 26454.

We used a KGW:Er-Yb single crystal for the luminescence experiments with a concentration of 1.20×10^{20} at./cm^3 for erbium and 4.16×10^{20} at./cm^3 for ytterbium.

In Er-Yb systems, the 1.5-μm emission of erbium obtained after selective ytterbium excitation can be attributed to an energy transfer process of erbium sensitized by ytterbium because of the energy overlap between them. This mechanism is schematized in Fig. 8. At selective Yb^{3+} excitation at 940 nm (10638 cm^{-1}), where no absorption of erbium takes place, excited electrons from the ground energy level of ytterbium to the $^2F_{5/2}$ excited energy level. After excitation, the electrons decayed radiatively to the ground state or transferred part of their energy to the $^4I_{11/2}$ energy level of erbium by cross relaxation. Once erbium was excited, the electrons decayed part radiatively, which

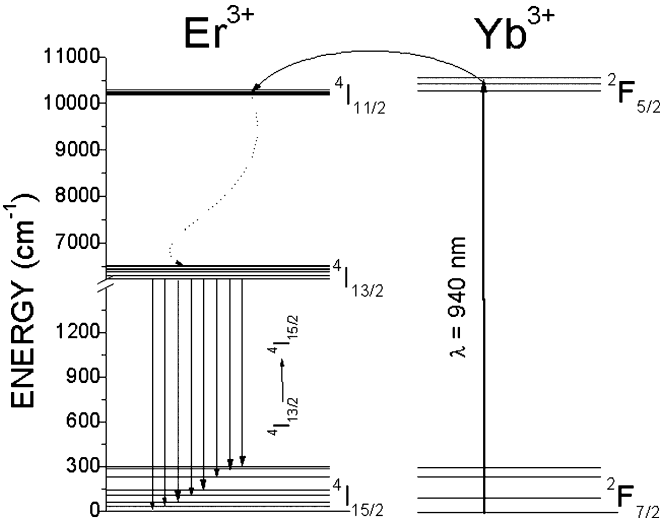

Fig. 8. Diagram of the implied energy levels of erbium and ytterbium ions in the energy transfer and the 1.5-μm emission of erbium in KGW:Er-Yb.

constitutes the 2.8-μm emission of erbium, and part nonradiatively to $^4I_{13/2}$ energy level. The population of the $^4I_{13/2}$ energy level decayed radiatively to the ground state, thus generating the 1.5-μm emission. The fact that part of the energy decayed nonradiatively from $^4I_{11/2}$ to $^4I_{13/2}$ was due to the small energy gap between these two energy levels. In fact, the energy gap was around 3600 cm^{-1} and, as the maximum phonon energy of KGW was 901 cm^{-1} obtained from Raman experiments [23], we may deduce the combination of four lattice phonons that relax nonradiatively from $^4I_{11/2}$ to $^4I_{13/2}$. This phenomenon was found in other erbium-doped hosts as in $LaLiP_4O_{12}$ glass [14].

Fig. 9 shows the 6 K emission spectrum for the $^4I_{13/2} \rightarrow {}^4I_{15/2}$ transition. The number of energy sublevels of the ground energy level expected by the crystalline field into the maximum number of Kramers levels is eight. The spectrum shows these eight transitions from the lower sublevel of the excited level

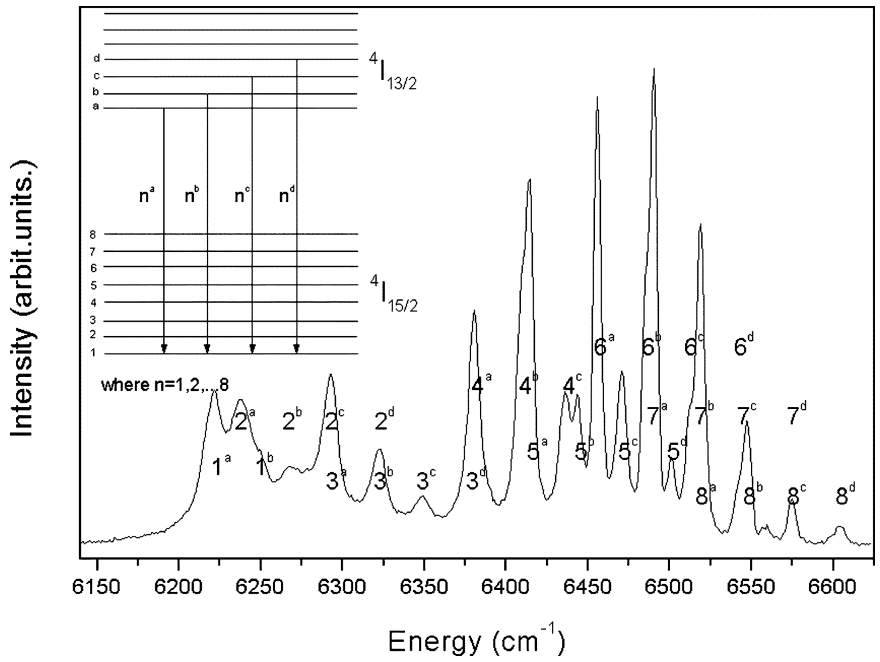

Fig. 9. High-resolution 1.5-μm emission of erbium performed at 6 K after pumping at 940 nm (10638 cm^{-1}).

TABLE III
SPLITTING OF THE EXCITED ENERGY LEVELS OF ERBIUM AND YTTERBIUM INVOLVED IN THE ENERGY TRANSFER AND SPLITTING OF THE GROUND STATE OF THE TWO IONS IN KGW:Er, Yb

Host	Active ion	$^{2S+1}L_J$	Sublevel energy position (cm^{-1})
KGW	Er	$^4I_{11/2}$	10197, 10223, 10237, 10267, 10290, 10296
		$^4I_{15/2}$	0, 29, 64, 105, 139, 227, 282, 298
	Yb	$^2F_{5/2}$	10196, 10487, 10686.
		$^2F_{7/2}$	0, 163, 385, 535.

to the first sublevel of the ground state and are represented by n^a $(n = 1,2,\ldots, ,8)$ in the spectrum. The energy values of these eight signals were 6519, 6490, 6455, 6414, 6380, 6292, 6237, and 6221 cm^{-1}. Moreover, it shows also some minor peaks that may be related to the transition from the three upper sublevels of the excited level to the lower sublevel of the ground state. These peaks are displaced in accordance with the difference in energy between the sublevels of the excited $^4I_{13/2}$; $\Delta E = 30$ cm^{-1} for the first and second sublevels increasing in energy, labeled n^b; $\Delta E = 57$ cm^{-1} for the first and third sublevels, n^c; and $\Delta E = 86$ cm^{-1} for the first and fourth sublevels, labeled n^d. The inset of Fig. 9 only shows the transitions from the lower sublevel of the excited level to the lower sublevel of the ground state. The value of n is each sublevel of the ground state. From the energy positions of the $^4I_{13/2}$ sublevels, and by substracting the above-mentioned energy values of emission signals, we found the energy positions of the energy sublevels of the ground state. These were 298, 282, 227, 139, 105, 64, 29, and 0 cm^{-1}, which were very close to those published in other tungstate matrices such as KYW and KErW [24]. From the low-temperature absorption measurements, the transition between the first sublevel of $^4I_{15/2}$ and the first sublevel of $^4I_{13/2}$ was 6517 cm^{-1}, and from the emission spectrum the value was 6519 cm^{-1}. This was due to the Stokes shift by the electron-phonon coupling. We considered that these values were absolutely the same, and, to calculate the energy position of the sublevels of the ground state, we used the value provided by the emission spectrum. Table III shows the energy position of the Stark energy levels of erbium and ytterbium corresponding to the energy levels that overlap in energy and the ground state of the two ions.

We measured the time decay of the emission corresponding to the $^4I_{13/2} \rightarrow {}^4I_{15/2}$ transition at 1.534 μm (6519 cm^{-1}) at several erbium and ytterbium concentrations in KGW:Er-Yb single crystals. To study the lifetime of the $^4I_{13/2}$ level and its dependence on the Yb^{3+} concentration, we performed the experiment on KGW:Er-Yb samples by fixing the erbium concentration and increasing the ytterbium concentration and by fixing the ytterbium concentration and increasing the erbium concentration. We achieved the decay profile of the infrared luminescence signal by exciting the sample resonantly to ytterbium at 940 nm (10638 cm^{-1}) and fixing the monochromator at the wavelength of the maximum emission at 1.534 μm (6519 cm^{-1}). Table IV shows the observed lifetimes and the concen-

TABLE IV
LIFETIME OF THE $^4I_{13/2}$ LEVEL OF ERBIUM AT SEVERAL DOPANT CONCENTRATIONS

Er,Yb concentration (%)	Lifetime (ms)
0.5,0.5	2.87
0.5,7.5	2.36
0.5,10	2.21
2.5,2.5	2.42
2.5,5.0	1.98
2.5,7.5	1.81
0.5,7.5	2.36
1.5,7.5	2.21
2.5,7.5	1.81

tration of ions of each measured sample. Significant changes in these values can be observed. When the erbium concentration was fixed and the ytterbium concentration increased, the lifetime of the $^4I_{13/2}$ energy level decreased due to the increase of the up-conversion process. This was consistent with the lifetime measurements of the green emission of erbium in KGW [25]. Moreover, when we fixed the ytterbium concentration and increased the erbium concentration, the lifetime also decreased due to the cross relaxation between erbium ions that resulted in a decrease of the lifetime.

IV. CONCLUSION

We successfully grew Er-Yb-doped $KGd(WO_4)_2$ single crystals with several concentrations of erbium and ytterbium ions by the TSSG method. We performed the spectroscopic characterization of erbium in this host in terms of the polarized optical absorption and luminescence at RT and 6 K. We payed attention to the characterization of the 1.5-μm (6667 cm^{-1}) emission and measured the lifetime at RT for several ytterbium concentrations.

From the polarized RT optical absorption measurements, we calculated the stimulated emission cross section using the Reciprocity method. Our results agree very well with those in the literature for similar tungstate hosts. We could therefore calculate the optical gain for several population inversion rates and determine the spectral region in which light amplification is possible for future laser experiments using this material for infrared emission.

From the polarized optical absorption measurements at 6 K, we determined the energy position of the sublevels of each excited energy levels. These energy positions, compared with those of other tungstate hosts, provide information about the influence of the crystal field of these hosts. Other parameters such as the Judd–Ofelt parameters for each tungstate and the distance between rare-earth ions confirmed the influence of the crystal field.

From the 6 K optical emission of the $^4I_{13/2} \rightarrow {}^4I_{15/2}$ transition of erbium, we found the energy position of the sublevels of the ground level. These results also agree very well with those in the literature for similar tungstate hosts.

From the lifetime measurements of the $^4I_{13/2}$ energy level of erbium for several erbium and ytterbium concentrations, we found that the increase of the erbium or ytterbium ions produced a decrease of the lifetime. Moreover, the $^4I_{13/2}$ energy level presented a very long lifetime that show us that easy population inversion is expected, which is needed for the generation of laser radiation.

ACKNOWLEDGMENT

The authors would like to thank the staff of Serveis Científico-Tècnics of the University of Barcelona (U.B.) for the EPMA measurements.

REFERENCES

[1] T. Schweizer, T. Jensen, E. Heumann, and G. Huber, "Spectroscopic properties and diode pumped 1.6 μm laser performance in Yb-codoped Er:$Y_3Al_5O_{12}$ and Er:Y_2SiO_5," *Opt. Commun.*, vol. 118, pp. 557–561, 1995.

[2] J. F. Digonnet, *Rare Earth Doped Fiber Lasers and Amplifiers*. New York: Dekker, 1993.

[3] W. Koechner, *Solid-State Laser Engineering*, 5th ed. Berlin, Germany: Springer-Verlag, 1999.

[4] R. C. Powell, *Physics of Solid-State Laser Materials*. Berlin, Germany: Springer-Verlag, 1998.

[5] S. Taccheo, P. Laporta, S. Longhi, O. Svelto, and C. Svelto, "Diode-pumped bulk erbium-ytterbium lasers," *Appl. Phys. B*, vol. 63, pp. 425–436, 1996.

[6] P. Klopp, U. Griebner, V. Petrov, X. Mateos, M. A. Bursukova, M. C. Pujol, R. Solé, Jna. Gavaldà, M. Aguiló, F. Güell, J. Massons, T. Kirilov, and F. Díaz, "Laser operation of the new stoichiometric crystal $KYb(WO_4)_2$," *Appl. Phys. B*, vol. 74, pp. 185–189, 2002.

[7] A. A. Kaminskii, K. Ueda, H. E. Eichler, J. Findeisen, S. N. Bagayev, F. A. Kuznetsov, A. A. Pavlyuk, G. Boulon, and F. Bourgeois, "Monoclinic tungstates $KDy(WO_4)_2$ and $KLu(WO_4)_2$-new $\chi^{(3)}$-active crystals for laser Raman shifters," *Jpn. J. Appl. Phys.*, vol. 37, pp. L923–L926, 1998.

[8] A. A. Kaminskii, *Crystalline Lasers: Physical Processes Operating Schemes*. Boca Raton, FL: CRC Press, 1996.

[9] M. C. Pujol, R. Solé, J. Massons, Jna. Gavaldà, X. Solans, C. Zaldo, F. Díaz, and M. Aguiló, "Structural study of monoclinic $KGd(WO_4)_2$," *J. Appl. Cryst.*, vol. 34, pp. 1–6, 2001.

[10] M. C. Pujol, M. Rico, C. Zaldo, R. Solé, V. Nikolov, X. Solans, M. Aguiló, and F. Díaz, "Crystalline structure and optical spectroscopy of Er^{3+}-doped $KGd(WO_4)_2$ single crystals," *Appl. Phys. B*, vol. 68, pp. 187–197, 1999.

[11] M. C. Pujol, R. Solé, V. Nikolov, Jna. Gavaldà, J. Massons, C. Zaldo, M. Aguiló, and F. Díaz, "Growth and ultraviolet optical properties of $KGd_{1-x}RE_x(WO_4)_2$ single crystals," *J. Mat. Res.*, vol. 14, pp. 3739–3745, 1999.

[12] R. Solé, V. Nikolov, X. Ruiz, Jna. Gavaldà, X. Solans, M. Aguiló, and F. Díaz, "Growth of $\beta - KGd_{1-x}Nd_x(WO_4)_2$ single crystals in $K_2W_2O_7$ solvents," *J. Cryst. Growth*, vol. 169, pp. 600–603, 1996.

[13] S. A. Payne, L. L. Chase, L. K. Smith, W. L. Kway, and W. F. Krupke, "Infrared cross-section measurements for crystals doped with Er^{3+}, Tm^{3+}, and Ho^{3+}," *IEEE J. Quantum Electron.*, vol. 28, pp. 2619–2630, Nov. 1992.

[14] A. F. Obaton, C. Parent, G. Le Flem, P. Thony, A. Brenier, and G. Boulon, "$Yb^{3+} - Er^{3+}$-codoped $LaLiP_4O_{12}$ glass: a new eye-safe laser at 1535 nm," *J. Alloys Comp.*, vol. 300–301, pp. 123–130, 2000.

[15] G. N. Van den Hoven, J. A. van der Elsken, A. Polman, C. van Dam, L. W. M. van Uffelen, and M. K. Smit, "Absorption and emission cross section of Er^{3+} in Al_2O_3 waveguides," *Appl. Opt.*, vol. 36, pp. 3338–3341, 1997.

[16] J. F. Philipps, T. Töpfer, H. Ebendorff-Heidepriem, D. Ehrt, and R. Sauerbrey, "Spectroscopic and lasing properties of Er^{3+} : Yb^{3+}-doped fluoride phosphate glasses," *Appl. Phys. B*, vol. 72, pp. 399–405, 2001.

[17] M. C. Pujol, M. A. Bursukova, F. Güell, X. Mateos, R. Solé, Jna. Gavaldà, M. Aguiló, J. Massons, F. Diaz, P. Klopp, U. Griebner, and V. Petrov, "Growth, optical characterization, and laser operation of a stoichiometric crystal $KYb(WO_4)_2$," *Phys. Rev. B*, vol. 65, p. 165 121, 2002.

[18] N. V. Kuleshov, A. A. Lagatsky, A. V. Podlipensky, and V. P. Mikhailov, "Pulsed laser operation of Yb-doped $KY(WO_4)_2$ and $KGd(WO_4)_2$," *Opt. Lett.*, vol. 22, pp. 1317–1319, 1997.
[19] X. Mateos, M. C. Pujol, F. Güell, R. Solé, Jna. Gavaldà, M. Aguiló, F. Díaz, and J. Massons, "Sensitization of Er^{3+} emission at 1.5 μm by Yb^{3+} in $KYb(WO_4)_2$ single crystals," *Phys. Rev. B*, vol. 66, p. 214 104, 2002.
[20] N. V. Kuleshov, A. A. Lagatsky, A. V. Podlopensky, V. P. Mikhailov, A. A. Kornienko, E. B. Dunina, S. Hartung, and G. Huber, "Fluorescence dinamics, excited-state absorption, and stimulated emission of Er^{3+} in $KY(WO_4)_2$," *J. Opt. Soc. Amer. B*, vol. 15, pp. 1205–1212, 1998.
[21] B. Z. Malkin, A. A. Kaminskii, N. R. Agalmayan, L. A. Bumagina, and T. I. Butaeva, "Spectra of rare-earth ions in the crystal fields of double tungstates and molybdates," *Phys. Stat. Sol. (b)*, vol. 110, pp. 417–422, 1982.
[22] M. C. Pujol, X. Mateos, R. Solé, J. Massons, Jna. Gavaldà, X. Solans, F. Díaz, and M. Aguiló, "Structure, crystal growth and physical anisotropy of $KYb(WO_4)_2$, a new laser matrix," *J. Appl. Cryst.*, vol. 35, pp. 108–112, 2002.
[23] J. Findeisen, H. J. Eichler, and A. A. Kaminskii, "Efficient picosecond $PbWO_4$ and two-wavelength $KGd(WO_4)_2$ Raman lasers in the IR and visible," *IEEE J. Quantum Electron.*, vol. 35, pp. 173–178, Feb. 1999.
[24] A. A. Kaminskii, *Laser Crystals, Their Physics and Properties*, 2nd ed. Berlin, Germany: Springer-Verlag, 1990, vol. 14, Opt. Sci..
[25] X. Mateos, C. Pujol, R. Solé, Jna. Gavaldà, M. Aguiló, F. Díaz, and J. Massons, "Infrared-to-green up-conversion in Er^{3+}, Yb^{3+}-doped monoclinic $KGd(WO_4)_2$ single crystals," *Opt. Mat.*, to be published.

Xavier Mateos was born in Tarragona, Spain, in 1975. He received the B.Sc. degree in chemistry from Rovira i Virgili University (U.R.V.), Tarragona, Spain, in 1997, where he is currently working toward the Ph.D. degree in chemistry.

His current work focuses on crystal growth, optical spectroscopy, and laser action of lanthanide-doped $KRE(WO_4)_2$ single crystals.

Maria Cinta Pujol was born in Reus, Spain, in 1973. She received the Ph.D. degree in chemistry from the Rovira i Virgili University (U.R.V.), Tarragona, Spain, in 2001. Her dissertation concerned growth and characterization of monoclinic crystals of $KGd(WO_4)_2$ modified with lanthanides.

Her research work includes crystal growth of single crystals and their structural and optical characterization, ceramic preparation, and structural, thermal, and mechanical characterization.

Frank Güell was born in Vila-Rodona, Spain, in 1973. He received the B.Sc. degree in physics from Barcelona University, Barcelona, Spain, in 1998, and he is currently working toward the Ph.D. degree in physics at the Rovira i Virgili University (U.R.V.), Tarragona, Spain.

Miguel Galán was born in Barcelona, Spain, in 1958. He received the B.Sc. degree in physics from Fachhochschule Ruesselsheim, Ruesselsheim, Germany, in 1985.

Currently he is working on development of laser diodes and solid-state lasers.

Rosa Maria Solé was born in Tarragona, Spain, in 1965. She received the Ph.D. degree in physics from Barcelona University, Barcelona, Spain, in 1994.

She is currently a Lecturer of applied physics with the Rovira i Virgili University (U.R.V.), Tarragona, Spain. Her research interests include phase diagrams, crystals growth, and physical properties of the solutions and crystals.

Josefina Gavaldà received the Ph.D. degree in physics from Barcelona University, Barcelona, Spain, in 1989.

Currently, she is a Senior Lecturer of applied physics with the Rovira i Virgili University (U.R.V.), Tarragona, Spain. She is working on optical spectroscopy of rare-earth ions for laser applications and on the morphological characterizations of several materials based in scanning electron microscopy.

Magdalena Aguiló was born in Sa Pobla, Mallorca, Spain, in 1953. She received the Ph.D. degree in physics from Barcelona University, Barcelona, Spain, in 1983.

Currently, she is a Professor of Crystallography with the Rovira i Virgili University (U.R.V.), Tarragona, Spain. Her research interests include crystal growth, X-ray diffraction, X-ray texture analysis, and physical properties in relation to the crystalline structure.

Jaume Massons was born in Lleida, Spain, in 1959. He received the Ph.D. degree in physics from Barcelona University, Barcelona, Spain, in 1987.

He is currently a Senior Lecturer of Applied Physics with the Rovira i Virgili University (U.R.V.), Tarragona, Spain. His research interests include optical spectroscopy of rare-earth ions for laser applications and nonlinear optical processes, such as cooperative luminescence and step-up conversion.

Francesc Díaz was born in Lugo, Spain, in 1953. He received the Ph.D. degree in physics from Barcelona University, Barcelona, Spain, in 1982.

Currently, he is a Professor of Applied Physics with the Rovira i Virgili University (U.R.V.), Tarragona, Spain. His research interests include optical spectroscopy (absorption and emission) of rare-earth ions for laser applications and nonlinear optical processes, such as cooperative luminescence and step-up conversion.